FRINGE 96
Accuracy of INSAR Measurements in Forested Areas

Patrik B.G. Dammert Department of Radio and Space Science
Chalmers University of Technology
S-412 96 GOTHENBURG, Sweden
dammert@rss.chalmers.se
http://www.rss.chalmers.se

Abstract

A large part of world is covered by boreal forest. As forest usually have low coherence, it is interesting to see how accurate INSAR-derived DEMs can be in forested areas. Both to see how the low coherence increases the noise in the DEM and to see how the forest will contribute to the DEM height. Different coherence measures are reviewed and DEM compensated coherence is found to the best. It has the lowest bias and standard deviation. Whenever a DEM is not available any knowledge of the topography improves the coherence estimation. However, without a DEM, coherence can both be underestimated and overestimated. For good land cover classification from coherence maps and analysis of INSAR-derived DEMs, a high-quality DEM from another source is preferred. An INSAR-derived DEM from an area in Sweden covered partly with boreal forest, has a total height RMS error for a 100x100 meter grid of around 5 meters. Of course, local RMS errors can be much higher depending on the local coherence. The three main problems in this case are height outliers over open water lakes, frozen lakes (ice-covered) can be on any level and the height bias caused by forests (in this case up to around 8 meters). Problems can partly be solved by averaging several interferometric DEMs, outliers will decrease or fully disappear. Unfortunately, the height bias over forests will only stabilize to a certain value, in this case to around 4 meters. For a five-pair interferometric DEM the total RMS error for a 100x100 meter grid was around 3.5 meters with maximum height errors up to 21 meters.

Keywords: SAR interferometry, DEM accuracy, coherence estimation, estimation bias

Introduction

C-band repeat-pass interferometric measurements from the satellites ERS-1 and ERS-2 have produced several interesting applications, *e.g.* DEM production, tree height measurements, glacier movements and earthquake measurements (see for example Goldstein et al. 1993, Massonnet et al. 1993, Zebker et al. 1994). Particularly DEM production is considered with high interest since a large part of the world does not have good and accurate DEMs and the interferometric SAR technique is very promising to overcome this lack of DEMs. Unfortunately, in the repeat-pass case the imaged ground has to be very stable between acquisitions to preserve the coherence in the image and that is almost only found in areas with dry rock and ground, *e.g.* deserts. The interferometric coherence is an important parameter determining how accurate the interferometric measurements are. For example, over forested terrain in Sweden (Ulander et al. 1993, Dammert et al. 1995, Hagberg et al. 1995) the coherence is usually very low but it is still possible to make measurements. Over forested terrain it is also important to investigate how the trees will contribute to the phase measurements. Measurements have earlier shown that the phase bias caused by forests is a complex function of tree and ground coherence, density of the trees and the tree height itself (Askne et al. 1995).

As a large part of the northern hemisphere is covered with boreal forest, it is interesting to see how good an INSAR-derived DEM corresponds to the real terrain height in such areas. It is also interesting to see how the accuracy of an INSAR-derived DEM corresponds with RMS errors predicted to be around 5 meters by (Zebker et al. 1994) and 1.7 meters by (Hagberg and Ulander 1993) (the difference in predictions are due to the different methods deployed in the articles). Large areas in Sweden are covered with forests which makes the problem more difficult since forests usually give rise to low coherence. In order to assess a INSAR-derived DEM, a good estimate of the coherence must first be determined. High coherence is easy to estimate but for low coherence the estimate is contaminated with a bias. This paper is divided into two main sections, one dealing with coherence estimation and the other with accuracy of INSAR-derived DEMs.

Interferometric data model

The two interferometric signals, *g1* and *g2*, can be considered determined from

$$\begin{cases} g_1 = a + b \\ g_2 = a e^{j\phi} + c \end{cases} \quad (1)$$

where *a*, *b* and *c* are independent circular complex Gaussian random variables distributed as ~ $CN\left(0, \sigma^2_{a,b,c}\right)$ and ϕ is the phase related to ground topography in the scene. The interferometric coherence is then defined as (Born and Wolf 1980)

$$\gamma = \frac{E\left\{g_1 g_2^*\right\}}{\sqrt{E\left\{|g_1|^2\right\} E\left\{|g_2|^2\right\}}} \quad (2)$$

where *E*{ } denotes expectation value. As coherence is an important parameter in interferometric SAR, it has to be estimated correctly.

Maximum likelihood coherence estimation

The maximum-likelihood, ML, estimator of the coherence for the model in Equation 1, with no ground induced phase, can be shown to be (Seymour and Cumming 1995)

(3)

$$\hat{\gamma} = \frac{\left|\sum_{i=1}^{N} g_{1,i} g_{2,i}^{*}\right|}{\sqrt{\sum_{i=1}^{N}|g_{1,i}|^2 \sum_{i=1}^{N}|g_{2,i}|^2}}$$

where *N* is the number of pixels. The estimate is only unbiased for asymptotically large datasets. However, the estimator's statistical properties are known (Tough et al. 1995, Touzi et al. 1996). Using the scheme in (Touzi et al. 1996) it is possible, given the mean of several coherence estimates, to retrieve the true coherence.

Equation 2 is, however, not valid when we have a topography-induced phase in the data, which is normally the case for INSAR images. The coherence ML estimator is then slightly revised as

$$\hat{\gamma} = \frac{\left|\sum_{i=1}^{N} g_{1,i} g_{2,i}^{*} e^{-j\theta_i}\right|}{\sqrt{\sum_{i=1}^{N}|g_{1,i}|^2 \sum_{i=1}^{N}|g_{2,i}|^2}} \tag{4}$$

where $e^{-j\theta_i}$ is a ground topography correction factor. In other words, ML estimation requires that the topography-induced phase is removed. Note that the fully topography-phase corrected coherence estimator (above) has exactly the same statistics as the estimator in Equation 3.

Insar coherence estimation

Using a DEM from another source is common for topography-correction of normal SAR intensity images and can also be used for coherence estimation as the topography-correction for the interferometric data. This leaves the interferometric coherence estimation as described in Equation 4 above.

On the other hand, if a DEM of the ground is not available, which normally is the case we must make an assumption about the ground topography. The topography-induced phase can be assumed to be constant, linear, quadratic or higher-order function over the estimation window. If the topography-induced phase is assumed to be constant over the whole estimation window, the estimator above will in practise look as the one in Equation 2. Note that the statistics of this estimator (let us call this estimator $\hat{\gamma}_0$) are not the same as those of the estimator in Equation 3, unless the true topography is constant over the estimation window.

If ground topography is assumed to change linearly over the estimation window, the coherence estimator corrects for a ground plane in the interferometric data as

$$\hat{\gamma}_1 = \frac{\max\limits_{\text{w.r.t. } \nu} \left|\sum_{i=1}^{N} g_{1,i} g_{2,i}^{*} e^{-j\nu i}\right|}{\sqrt{\sum_{i=1}^{N}|g_{1,i}|^2 \sum_{i=1}^{N}|g_{2,i}|^2}} \tag{5}$$

where $e^{-j\nu i}$ denotes the ground topography correction factor and it can also be seen as a Fourier kernel. The coherence is found locating the highest peak in the spectral domain. This procedure will give a higher bias as it reduces the variance and independent number of samples in the data and it will find the wrong values for low coherence values (the spectrum will be whiter as the coherence drops). However, a sufficiently large number of samples in the estimate will make it possible to measure low coherences.

For small estimation windows, the phase can in practise always be assumed to be linear. For larger estimation windows or steep terrain, it may on the other hand be necessary to correct for quadratic phase values, *i.e.*

$$\hat{\gamma}_2 = \frac{\max\limits_{\text{w.r.t. } \nu \text{ and } p} \left|\sum_{i=1}^{N} g_{1,i} g_{2,i}^{*} e^{-j\nu i - jpi^2}\right|}{\sqrt{\sum_{i=1}^{N}|g_{1,i}|^2 \sum_{i=1}^{N}|g_{2,i}|^2}} \tag{6}$$

or even cubic phase values in the data. Of course, higher-order corrections will reduce the dataset variance more and the bias of the estimator will not decrease leaving low coherence measurements still biased.

Some basic knowledge about the topography in the imaged scene will improve the assumptions. Very little and slowly varying topography, use linear phase correction. Steep and very varying topography, use parabolic phase correction or decrease the estimation window. For practical reasons although, phase is usually considered linear as this makes it possible to estimate the coherence by a Fourier transform, see Equation 5 above.

Using an imperfect assumption of the ground topography or a too large estimation window will result in a lower estimated coherence. Unresolved topographic variations, if they are assumed to be Gaussian, will lower the estimate as

(7)

$$\hat{\gamma} \propto \exp\left(-\frac{1}{2}\left(\frac{4\pi b_n}{\lambda R \sin\theta}\sigma_h\right)^2\right)$$

where σ_h denotes unresolved topographic RMS variations. Equation 7 is also valid for evaluating topographic variations inside a resolution cell. As illustrated in Figure 1, the effect is small for short baselines. Figure 1 also illustrates the fact that for long baselines and large topographic variations the estimated coherence will be practically zero while the coherence using topography-correction could actually be one. In steep terrain this can be true, on the other hand steep terrain is often related to other problems such as layover and shadow effects.

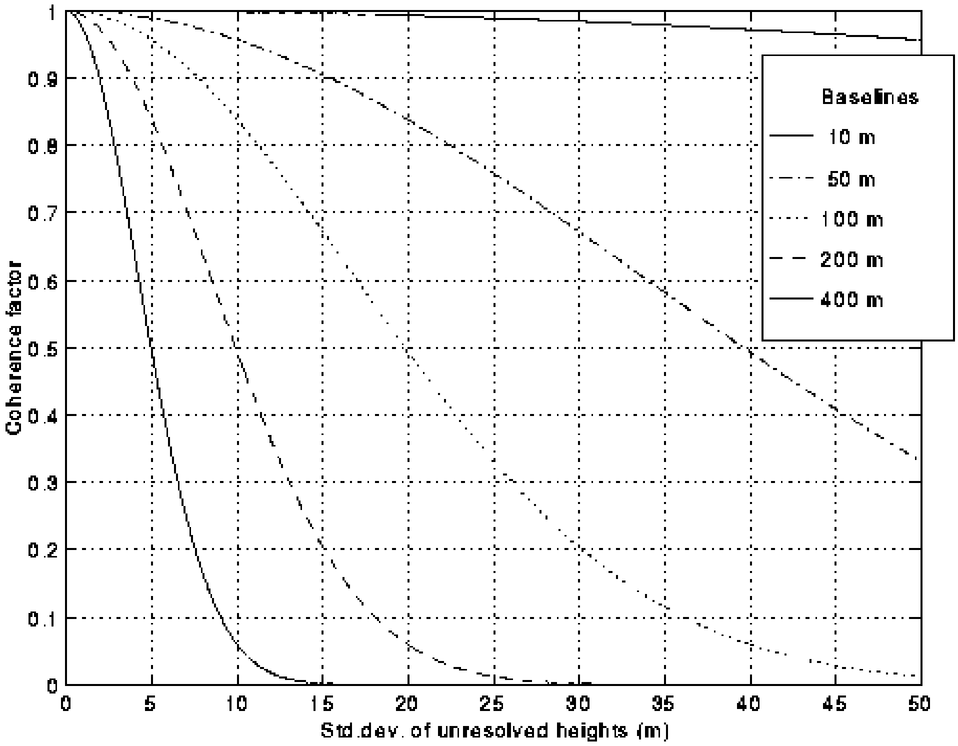

Figure 1. Coherence factor due to unresolved topographic variations. ERS-1 system parameters are used.

Other coherence estimators

A simple case occurs when the power is known *a priori* in the interferometric dataset. In this case, it leaves the coherence ML estimation as

$$\hat{\gamma}_3 = \frac{1}{\sigma_{g1}\sigma_{g2}N}\left|\sum_{i=1}^{N} g_{1,i}g_{2,i}^{*}\right| \tag{8}$$

where σ_{g1} and σ_{g2} are the powers of the two signals respectively. As the estimate includes only the magnitude this will lead to a biased estimator. Following the p.d.f. in (Lee et al. 1994) and the integral tables in (Gradshteyn and Ryzhik 1994) it is possible to calculate the expected value of this estimator as

$$E\{\hat{\gamma}_3\} = \frac{\sqrt{\pi}\left(1-\gamma^2\right)^{N+1}\Gamma(N+1/2)}{2\Gamma(N)} F\left(\frac{3}{2}, N+\frac{1}{2}; 1; \gamma^2\right) \tag{9}$$

where $\Gamma()$ is the Gamma function and $F(;;;)$ is the hypergeometric function. Comparison between the above estimator and the ML estimator (Equation 3) yields that the above estimator is slightly better for low coherence. Moreover, information about image statistics *a priori* is not very likely, but determining power from a large homogenous area in the image will yield a good estimate with a small confidence interval. This will leave a coherence estimation with information nearly *a priori*. This procedure can be exploited for real interferograms but with the problem of how to determine homogeneous areas.

A "quick-and-dirty" coherence estimator has been derived by the group at POLIMI in Italy (Gatelli et al. 1996). It is intended for selection of interferometric pairs with good coherence as its implementation is quick. This estimator is included in this study for interest only and is described as

$$\hat{\gamma}_4 = \begin{cases} \sqrt{2\hat{\rho}-1} & \hat{\rho} > \frac{1}{2} \\ 0 & \hat{\rho} \le \frac{1}{2} \end{cases} \tag{10}$$

where $$\hat{\rho} = \frac{\sum_{i=1}^{N} |g_{1,i}|^2 |g_{2,i}|^2}{\sqrt{\sum_{i=1}^{N} |g_{1,i}|^4 \sum_{i=1}^{N} |g_{2,i}|^4}}$$

Note that the phase is not used in this estimator. As this coherence estimator can be derived from the higher-order moments of the combined p.d.f. of the interferometric dataset, the variance of this higher-order moment estimator is larger than the best moment estimator which is the same as the above ML estimator (see Equation 3).

Spectral whiteness

The spectral whiteness of a signal is defined as (Markel and Gray Jr 1976)

$$\Theta_x = \frac{\exp\left\{\int_{-1/2}^{1/2} \ln S_x(\upsilon) d\upsilon\right\}}{\int_{-1/2}^{1/2} S_x(\upsilon) d\upsilon} \qquad (11)$$

where Θ_x is the spectral whiteness and S_x is the spectrum for the stochastic signal *X*. The spectral whiteness will be unity for totally white signals and between zero and unity for more colored signals. As discussed above (under the assumption of a linear phase in the data), a low coherence dataset will have a white spectrum while higher coherence datasets will have more sharp peaks in their spectra (*i.e.* more colored spectra). Ideally, zero-coherence datasets should have unity spectral whiteness. Therefore it is interesting to see how the spectral whiteness varies with the coherence in the dataset.

Simulations

An evaluation of the different estimators was carried out through simulations using the interferometric model in Equation 1. The number of independent samples was chosen to be 50, which corresponds to approximately 5x25 pixels (=100x100 square meters on ground) for an ERS-1 interferogram. Two simulations were carried out, one simulation with the topography-induced phase set to zero and one with a real DEM-modulated phase.

The first simulation (without a topography-induced phase) shows, as expected, that higher-order functions fitted to the phase increase the bias of the coherence estimates. Results are illustrated in Figure 2. However, the most interesting simulation is when the true coherence is zero as illustrated in Table 1. Simulations also validated the known statistics for the normal ML estimator (see Equation 3) as well as for the estimator with power *a priori* (see Equation 8). Note that the DEM-compensated estimator loses its relevance in this case.

The power *a priori* coherence estimator performs slightly better than the normal ML estimator, however, the difference is almost negligible. It is more critical that this estimator performs very poor for high coherence, *e.g.* large standard deviations and giving estimates larger than one. The POLIMI estimator performs poorly for low coherence, a high bias and a large standard deviation, while the high coherence estimates are accurate. This is expected as the purpose of this estimator is only selection of good interferometric pairs. It also shows that higher-order moment estimators for coherence is not the route to good low-coherence estimators.

Simulations for the spectral whiteness show a small variation depending on coherence. The zero coherence simulation which should have produced a spectral whiteness of unity, does instead produce a measure 0.5734. An explanation is that the dataset is finite, for an infinite dataset, the spectral whiteness would be unity. However, increasing the estimation window will reduce resolution and perhaps violate the linear-phase assumption. More or less, the simulations show that spectral whiteness is not a good discriminator for different coherence values.

Table 1 Performance of coherence estimates with true coherence set to zero. 10000 simulations.

Coherence estimator	Mean of simulation result	Std.dev. of simulations result	Mean - Std.dev.	Mean + Std.dev.
γ_0	0.1238	0.0640	0.0598	0.1878
γ_1	0.3191	0.0383	0.2808	0.3574
γ_2	0.4182	0.0322	0.3860	0.4504
γ_3	0.1232	0.0650	0.0582	0.1882
γ_4	0.2035	0.2068	~0	0.4103
Θ_x	0.5734	0.0447	0.5287	0.6181

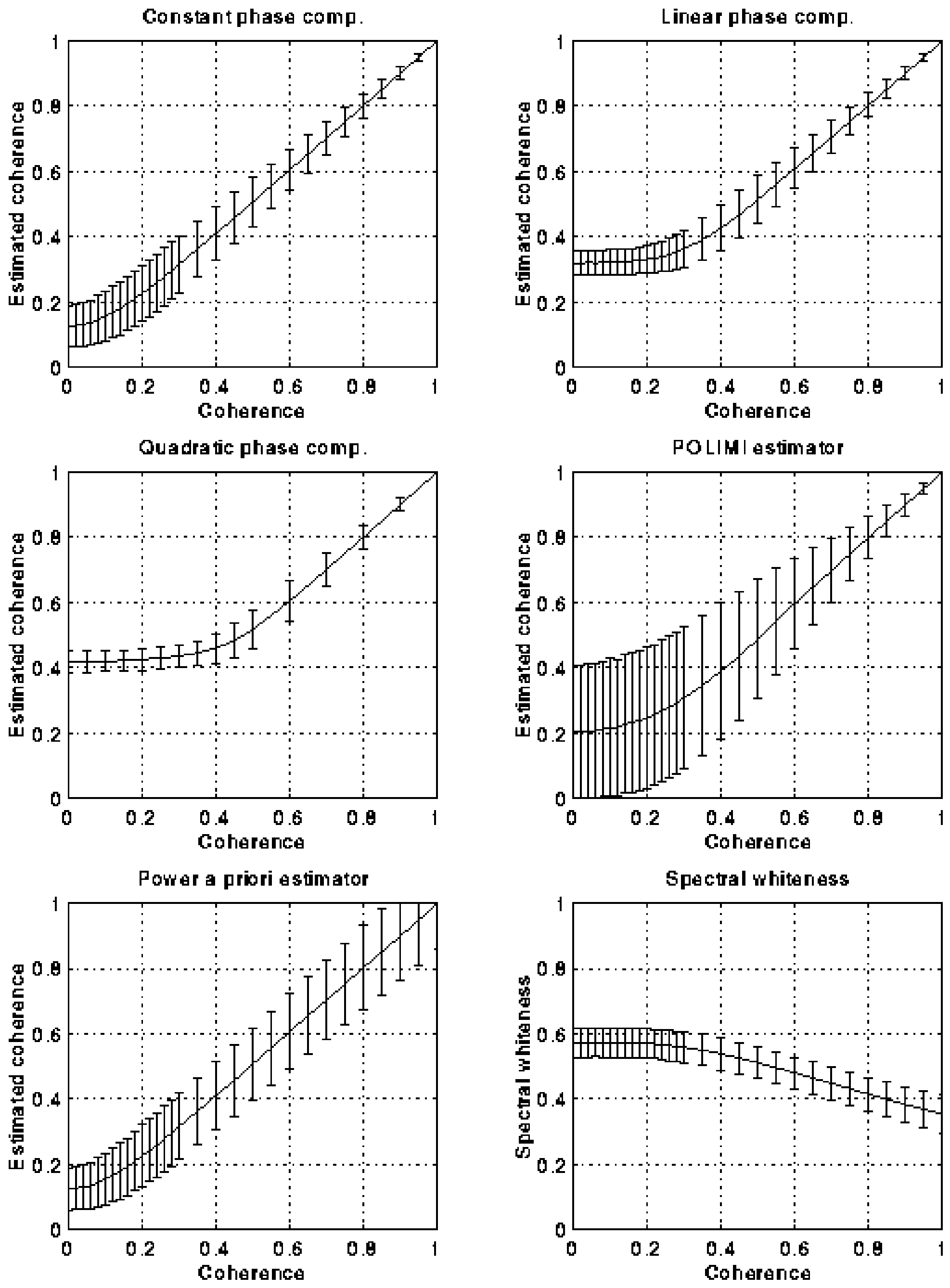

Figure 2. Simulations of the six coherence measures. The bars denote the standard deviations. Number of simulations 10000.

The simulations with a DEM-modulated phase show other interesting artefacts. The chosen DEM describes a rather flat coastland with some farmland scattered around but the main part of it is more hilly forested terrain. Highest mountain is around 200 meters high and maximum slope is never over 15 degrees. The interferometric phase is calculated with parameters equal to ERS-1 geometry and the true coherence is set to unity.

Results are found in Table 2. Simulations show that the power *a priori* coherence estimator performs very poor, it has a large standard deviation and can even give values above one. The spectral whiteness measure also seems to have a large estimation interval. Moreover, as expected the POLIMI estimator and the DEM corrected estimator performed best in this simulation. The other coherence estimators which give values below one is merely because there is unresolved topographic variations in the estimation window, *cf.* Equation 7 and Figure 1. It is also obvious why the linear-phase compensation performed better than the constant-phase compensation.

Table 2 Performance of coherence estimates with a topographic phase.

Coherence estimator	Mean of simulation result	Std.dev. of simulations result	Max. of simulation	Min. of simulation
γ_0	0.9937	0.0136	1	0.7958
γ_1	0.9971	0.0037	1	0.9738
γ_3	0.9944	0.0903	1.4325	0.6942
γ_4	1	0	1	1
DEM-corrected coherence	1	0	1	1
	0.3460	0.0328	0.2234	0.5670

Θ_X				

Coherence measurements from real images

For practical reasons, the constant- and linear-phase assumption coherence estimators together with the POLIMI estimator are often used because of the simple implementations, although for different purposes. Using a DEM as a phase correction is also straightforward, whenever such is available. Figure 3 illustrates the difference between the linear-phase assumption and with a DEM available for an existing interferometric pair. As the DEM corrected coherence estimates are believed to be best, the fitted line shows that the linear-phase assumption overestimates low coherence and underestimates high coherence. The overestimates for low coherence is explained by the definition and simulations (see sections above). However, the linear-phase compensated coherence estimator can always underestimate coherence, the effect is here clearly seen for high coherence. For low coherence, there can be both over- and underestimation of the coherence using the linear-phase compensation. The underestimates is an outcome of unresolved topographic variations in the estimation window which, of course, is there for both low and high coherence (*cf.* Equation 7). As the DEM-compensated coherence estimator performs better at all coherence values, reliable coherence measurements should be done with a DEM compensation. Moreover, looking at DEM compensated coherence maps, lakes are easier discriminated than in linear-phase compensated coherence maps.

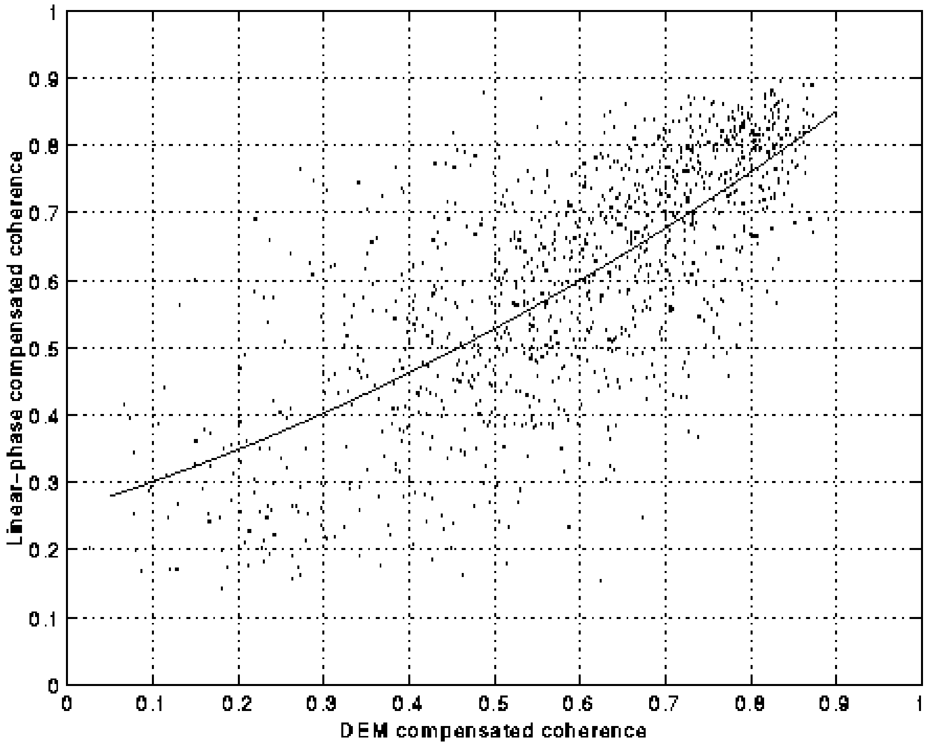

Figure 3 DEM compensated vs. linear-phase compensated coherence estimates, a line is fitted for visual aid. Part of the image pair no. 1 in Table 4.

Unfortunately, there is a problem over forested areas. The scattering centre in a forest is not at ground level (Ulander et al. 1993, Dammert et al. 1995, Hagberg et al. 1995, Small et al. 1995), so the DEM compensation is actually wrong over any kind of forest. The effect will be an underestimated coherence (as above), but the effect can be negligible if the RMS of the scattering centre height is small, *c.f.* Equation 7 and Figure 1. For our baselines and rather homogenous forests, the effect is therefore considered negligible in this paper.

Phase estimation

A reliable coherence measure is extremely important for evaluating the interferometric phase accuracy, *i.e.* the accuracy of an INSAR derived DEM. Given the interferometric model in Equation 1, the maximum-likelihood phase estimate is (Seymour and Cumming 1995)

$$\hat{\phi} = \arg\left(\sum_{i=1}^{N} g_{1,i}\, g_{2,i}'\right) \qquad (12)$$

which can be seen merely as the phase of the ML complex coherence estimator. The variance of this estimator is given by (see for example Lee et al. 1994)

$$\sigma_{\hat{\phi}}^2 = \frac{\Gamma(N+1/2)(1-\gamma^2)^N \gamma}{2\sqrt{\pi}\,\Gamma(N)} \int_{-\pi}^{\pi} \frac{\phi^2 \cos\phi}{(1-\gamma^2\cos^2\phi)^{N+1/2}}\, d\phi + \\ + \frac{(1-\gamma^2)^N}{2\pi} \int_{-\pi}^{\pi} \phi^2 F(N,1;1/2;\gamma^2\cos^2\phi)\, d\phi \qquad (13)$$

where $\Gamma()$ is the Gamma function and $F(,;;)$ is the hypergeometric function. Knowing the true coherence in an area, it is possible to calculate the variance of the phase estimate and thus the variance of the height measurement, *i.e.* the interferometric

DEM. Of course, the accuracy of the topographic height also depends on the accuracy of system parameters (for example such as interferometric baseline, incidence angle etc.), but they are believed to be negligible compared with the phase noise.

Accuracy of interferometric dems

A total of five interferometric pairs is included in the analysis, the pairs are described in Table 4. To assess the accuracy for an interferometric DEM over an area in northern Sweden covered partly with boreal forest, a comparison with a real DEM was made. However, to circumvent the difficult problem of phase unwrapping in low-coherence areas and exact geocoding of the interferogram, "synthetic" interferograms were simulated from the real DEM. By looking at the phase difference between the real and synthetic interferograms, it is possible to determine the accuracy of the interferometric DEM.

Table 4 Interferometric pairs used in this study.

Pair number	Acq. date 1	Acq. date 2	Normal baseline (m)
1	94-02-24	94-02-27	204
2	94-02-06	94-02-15	295
3	94-03-11	94-03-23	203
4	94-03-14	94-03-23	182
5	94-03-17	94-03-23	177

One-pair interferometric DEM

This analysis includes interferometric pair no. 1. Figure 4 illustrates the local RMS error of the interferometric DEM together with a predicted RMS error map derived according to Equation 13. The fact that the heavy multi-looked data display higher height differences than the theoretical values for a given coherence is probably caused by uncertainty of system parameters. As illustrated in Table 5, the accuracy of the interferometric DEM is quite bad for the 1-look, 5-look and 20-look cases. Only the 125-look case seems to give reasonable vertical resolution. However, looking at Figure 4 it is true that the worst values are around the same, but these values occur for low coherence. For high coherence values the vertical resolution improves. In other words, multi-looked interferometric DEMs improve the accuracy at high coherence but for low coherence the accuracy is approximately the same. The multi-look interferometric DEM is more accurate as expected, but horizontal resolution is traded off for improvement of vertical resolution.

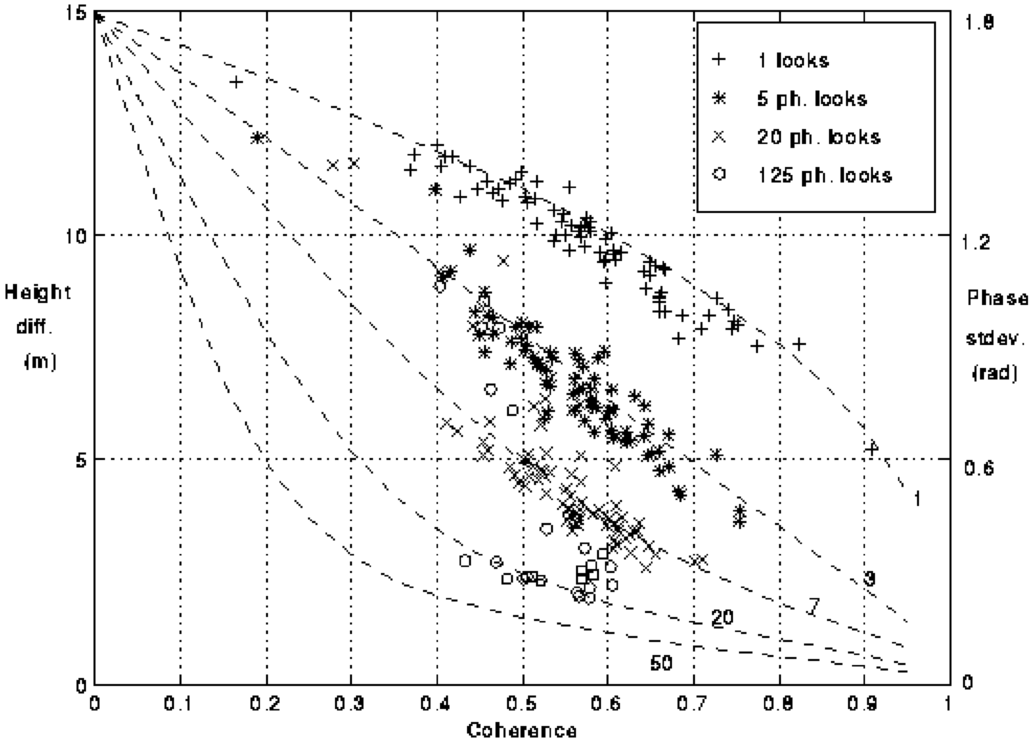

Figure 4 Local RMS error of the interferometric DEM. Dashed lines are the theoretical values given by Equation 13 for a certain number of independent looks (number of looks placed right of the lines). Right-hand y-axis displays the phase while the left-hand y-axis displays the corresponding heights. Note also the difference between independent and physical number of looks.

Table 5 Phase and height differences compared with different horizontal resolution.

No. of physical looks	Approx. ground area (m2)	Approx. no. of independent looks	Max. local RMS phase difference (rad)	Max local RMS height difference (m)
1	20 x 4	1	1.80	14.9
5	20 x 20	3	1.79	14.8
20	40 x 40	8	1.56	12.9
125	100 x 100	50	1.08	8.86

For the single pair DEM, one of the largest problem is the outliers caused by lakes and sea. For open water coherence is zero and the phase can thus take on any value. In this case with partly frozen lakes, another problem has occurred. The ice cover has moved coherently between acquisitions giving rise to a phase shift. For DEM production it means that the height of the lake can be on any level.

As pointed out in several papers (Ulander et al. 1993, Dammert et al. 1995, Hagberg et al. 1995, Small et al. 1995), a forest will cause a height bias in the interferometric DEM. Depending on circumstances and bole volume of a forest, the bias will be different. In this area, the interferometric height of a certain large homogeneous forest has been measured to 2.2 meters for this pair but can be higher for other pairs, see Table 6. Of course, the low coherence over forests gives rise to large height standard deviations as well. More multilooking will decrease the height standard deviation (*i.e.* decrease the phase noise).

A large part of this area is covered by forests, so an additional error caused by the trees is expected in the interferometric DEM. Part of the RMS error in the above interferometric DEM can thus be explained by forests in the scene.

Table 6 Measured forest heights for the image pairs (Askne et al. 1996).

Pair number	Forest mean height (m)	Forest std. dev. (m)
1	2.2	11.9
2	1.1	8.5
3	5.3	N/A
4	7.3	12.8
5	2.7	N/A

Multiple pair interferometric DEM

An average of the five interferometric DEMs, derived from the pairs in Table 4, was performed to decrease height errors. The errors should decrease as $1/\sqrt{M}$, where *M* is the number of independent measurements. As the interferometric forest height varies in different interferograms (*c.f.* Table 6), an average of several interferometric DEMs will also stabilize the height bias caused by forests. Nevertheless, a high RMS error will always exist over a forested area because of the low coherence. The result is illustrated in Table 7.

Table 7 Accuracy of one INSAR-pair DEM and a multiple INSAR-pair DEM.

		DEM derived from one pair		DEM derived from five pairs	
Number of physical looks	Approx. ground area (m2)	Total RMS height error (m)	Maximum height error (m)	Total RMS height error (m)	Maximum height error (m)
5	20 x 20	8.02	25.88	4.70	22.46
20	40 x 40	6.15	25.88	4.23	21.76
80	80 x 80	5.19	25.77	3.65	22.26
125	100 x 100	4.98	25.87	3.49	21.03

The maximum errors for the one-pair DEM corresponds actually to $\pm\pi$ radians in that interferogram, *i.e.* the maximum phase value in the interferograms. In the five-pair DEM RMS errors are decreased as expected, but more important is that outliers, seen in the one-pair DEM, seem to fully disappear. Moreover, the interferometric heights of frozen lakes are better than for the one-pair case. The error caused by a certain forest for this particular five-pair DEM is easily evaluated from measurements and is approx. 3.7 meters for this forest, see Table 6. Other forests are expected to have similar values, of course depending on forest density, actual tree height and other circumstances.

Conclusions

As already well known, coherence estimates are biased for low coherence measurements. Decreasing horizontal resolution will decrease the estimate's bias. As low coherence means a noisy signal, more data has to be averaged to get good measurements. Simulations show that DEM corrected coherence estimates outperforms those of any other estimator, both for low and high coherence. Simulations also show that even for quite moderate topography, the other estimates will be good, although for larger topography coherence will always be underestimated. To have a reliable coherence measure is important both for DEM production and land cover classification by coherence. Estimation with a DEM is therefore always preferred. Nevertheless, for DEM production there may not be a *a priori* DEM and in this case any basic knowledge about the topography will improve the coherence estimates. Furthermore, it is very hard to distinguish low coherence areas in this case.

The DEMs derived in this study, have generally rather low RMS height errors. However, they are worse than those predicted in (Hagberg and Ulander 1993, Zebker et al. 1994) which were 5 and 1.7 meters respectively. Of course, the RMS errors in this study include very low coherence values which could affect RMS errors in a negative way. For the single pair DEM, the largest problem is the outliers caused by lakes and sea. In this case with partly frozen lakes, another problem has occurred. The ice cover has moved coherently between acquisitions giving rise to a phase shift. For DEM production it means that the height of the lake can be on any level. With forests in the scene, there can be an additional height bias up to around 8 meters.

The multiple pair DEM shows a better RMS height error as expected. However, most noteworthy is that outliers over open water lakes have disappeared and the height bias caused by a certain forest is decreased to around 4 meters. Other forests are believed to cause similar height biases. Errors caused by coherent movements of ice in lakes are of course also decreased. The multiple pair DEM is much smoother than the one pair DEM.

Multiple pair DEMs will thus decrease errors caused by unfrozen lakes, frozen lakes and forests. The benefit going from one pair to several pairs is thus obvious. For DEM production, more than one pair is therefore needed, preferably a series of SAR images.

Future work should include areas with greater topography, perhaps even with layover and shadow effects, to see where the actual limit is for INSAR derived DEMs. As different interferometric DEMs have different SNRs (*i.e.* coherence) a minimum variance DEM average can be performed to decrease height errors even further. This should also be studied for future work. Of course, a good and stable phase unwrapping technique for low coherence areas also has to be developed.

Acknowledgements

I would like to acknowledge insights and valuable discussions with Prof. Jan Askne, at Chalmers, together with the new and good ideas and problem clarifications by Dr. Lars Ulander at FOA, Sweden. Ideas and help from Gary Smith and Prof. D. Rosenholm are also acknowledged. LMV, Sweden, is acknowledged for the DEM.

The research in this study is financed by a grant from the Swedish National Space Board.

References

Askne, J., Dammert, P. B. G., Fransson, J., Israelsson, H. and Ulander, L. M. H., 1995, Retrieval of forest parameters using intensity and repeat-pass interferometric SAR information, *Proceedings of Retrieval of Bio and Geophysical Parameters from SAR Data for Land Applications held in Toulouse, 10-13 October 1995*, ,

Askne, J., Dammert, P. B. G. and Smith, G., 1996, INSAR Application Evaluation Report: INSAR for Forest Mapping, Department of Radio and Space Science, Chalmers University of Technology, Gothenburg, Sweden.

Born, M. and Wolf, E., 1980, *Principles of Optics* (Pergamon Press).

Dammert, P. B. G., Ulander, L. M. H. and Askne, J., 1995, SAR Interferometry for Detecting Forest Stands and Tree Heights, *Proceedings of European Symposium on Satellite Remote Sensing II held in Paris, France, 25-28 September 1995*, ,

Gatelli, F., Monti Guarnieri, A., Prati, C. and Rocca, F., 1996, Medium Resolution Efficient Phase Preserving Focusing for Interferometry, *Proceedings of IGARSS'96 held in Lincoln, 27-31 May 1996*, ,

Goldstein, R. M., Engelhardt, H., Kamb, B. and Frolich, R. M., 1993, Satellite radar interferometry for monitoring ice sheet motion: application to an Antarctic ice stream, *Science*, **262,** 1525-1530.

Gradshteyn, I. S. and Ryzhik, I. M., 1994, *Table of Integrals, Series and Products* (Boston: Academic Press Inc.).

Hagberg, J. O. and Ulander, L. M. H., 1993, On the Optimization of Interferometric SAR for Topographic Mapping, *IEEE Transactions on Geoscience and Remote Sensing*, **31,** 303-306.

Hagberg, J. O., Ulander, L. M. H. and Askne, J., 1995, Repeat-Pass SAR Interferometry over Forested Terrain, *IEEE Transactions on Geoscience and Remote Sensing*, **33,** 331-340.

Lee, J., Hoppel, K. W., Mango, S. A. and Miller, A. R., 1994, Intensity and Phase Statistics of Mulitlook Polarimetric and Interferometric SAR Imagery, *IEEE Transactions on Geoscience and Remote Sensing*, **32,** 1017-1028.

Markel, J. D. and Gray Jr, A. H., 1976, *Linear Prediction of Speech* (New York: Springer Verlag).

Massonnet, D., Rossi, M., Carmona, C., Adragna, F., Peltzer, G., Feigl, K. and Rabaute, T., 1993, The Displacement Field of the Landers Earthquake Mapped by Radar Interferometry, *Nature*, **364,** 138-142.

Seymour, M. and Cumming, I., 1995, Maximum Likelihood Estimation and Cramer-Rao Bounds for SAR Interferometry, Department of Electrical Engineering, University of British Columbia, Vancouver.

Small, D., Holecz, F. and Nüesch, D., 1995, Combination of Ascending / Descending ERS-1 INSAR Data for Calibration and Validation, *Proceedings of IGARSS'95 held in Firenze, 10-14 July 1995*, ,

Tough, R. J. A., Blacknell, D. and Quegan, S., 1995, A Statistical Description of Polarimetric and Interferometric Synthetic Aperture Radar Data, *Proceedings of the Royal Society, London*, **449,** 567-589.

Touzi, R., Lopes, A. and Vachon, P. W., 1996, Estimation of Coherence Functions for Interferometric SAR Applications, *Proceedings of EUSAR'96, 26-28 March 1996 held in Königswinter*, ,

Ulander, L. M. H., Hagberg, J. O. and Askne, J., 1993, ERS-1 SAR Interferometry over Forested Terrain, *Proceedings of Second ERS-1 Symposium Space at the Service of Our Environment held in Hamburg, 11-14 October 1993*, ,

Zebker, H. A., Werner, C. L., Rosen, P. A. and Hensley, S., 1994, Accuracy of Topographic Maps Derived from ERS-1 Interferometric Radar, IEEE Transactions on Geoscience and Remote Sensing, **32**, 823-836.